



The origin of fatigue fracture in single-crystal silicon

H. Izumi¹, T. Kita^{1,2}, S. Arai³, K. Sasaki^{3,4}, and Shoji Kamiya^{1,*}

¹Nagoya Institute of Technology, Gokiso-cho, Showa-ku, Nagoya 466-8555, Japan

²Kawasaki Heavy Industry, Kakamigahara 504-8710, Japan

³Nagoya University, Furo-cho, Chikusa-ku, Nagoya 464-8601, Japan

⁴UACJ Corporation, Nagoya 455-8670, Japan

Received: 10 September 2021

Accepted: 22 February 2022

Published online:

20 April 2022

© The Author(s), under exclusive licence to Springer Science+Business Media, LLC, part of Springer Nature 2022

ABSTRACT

Mechanical fatigue in silicon was discovered in 1992, but the mechanism by which it takes place has yet to be clarified. To determine the fatigue mechanism, a new testing structure was developed and optimized for investigation by high-voltage transmission electron microscopy (HVTEM). After 5×10^5 fatigue cycles at 25 °C and 80% relative humidity (RH), the entire thickness of the fractured specimen was examined directly by HVTEM without applying a thinning process, which eventually shaves off part of the material to be observed. The investigation revealed a number of line defects emanating from the stress concentration notch that accumulated on particular planes and also from the points beside the origin of the unstable crack extension. Those defects were identified as edge dislocations moving along the slip plane {111} in the slip direction $\langle 110 \rangle$, which is typical of the silicon slip system. Therefore, our findings strongly suggest that mechanical fatigue fracture takes place in silicon owing to dislocations moving under repeated loading, even at approximately 25 °C, i.e., room temperature, in the same way as in metallic materials.

Introduction

In the past, the mechanical fatigue of silicon has been a mystery. It has long been common knowledge that silicon is susceptible to fatigue fracture [1–4]. However, owing to its brittle fracture behavior at room temperature [5], it was considered unlikely that the crystal fatigue fractures were caused by subcritical defect growth and the actual cause has not really

been identified. This gap in knowledge was once filled by the hypothesis that the surface oxide layer, not the bulk crystal itself, was the key to fatigue fracture [6, 7]. It was claimed that the oxide layer was thickened by cyclic stress, was subjected to corrosion cracking in humid environments, and ultimately cracked apart together with the rest of the structure. This hypothesis was once taken seriously because it apparently explained the shorter fatigue lifetime of crystals in conditions of high humidity. However, the

Handling Editor: M. Grant Norton.

Address correspondence to E-mail: kamiya.shoji@nitech.ac.jp

<https://doi.org/10.1007/s10853-022-07055-5>

most important features of this hypothesis, i.e., the corrosion cracks in the thickened oxide layer, have been detected only once using high-voltage transmission electron microscopy (HVTEM) and have hardly ever been observed elsewhere. Moreover, the hypothesis did not provide an explanation for the growth of the oxide under cyclic stress, and the thick oxide layer observed was later speculated to be due to the fabrication process.

However, evidence of dislocation glide and plastic deformation in silicon at room temperature or even lower has been frequently reported. For example, indentation [8] and scratch [9] tests have revealed that so-called shuffle set dislocations can be introduced at temperatures as low as liquid nitrogen temperature, i.e., $-196\text{ }^{\circ}\text{C}$ (77 K). Dislocation emissions along unstable crack extensions are also common, even at approximately room temperature [10]. In small-scale structures such as narrow beams under bending stress [11, 12], or small pillars under compression [13–16], plastic deformation can be macroscopically identified by mechanical tests at room temperature. Even when the absolute scale of the plastic deformation is small, if it accumulates under cyclic fatigue loading, it can become large enough to trigger catastrophic fatigue fracture, as in metallic materials. Such a possibility was already suggested [17], whereby ultrasonic agitation at room temperature yielded a cluster of dislocations underneath a tungsten pillar standing on silicon in an electronic device. However, although it is a probable origin of fatigue fracture, crystal slip deformation has not been identified in normal fatigue tests. Accordingly, there is no direct evidence that fatigue fracture is caused by crystal slip deformation in silicon. Therefore, fatigue fracture has remained a mystery in silicon, even though it poses a serious threat to the reliability of silicon structures in microscale sensors and actuators (so-called microelectromechanical systems (MEMS)).

Why are crystal defects rarely found during fatigue or even after fatigue fracture? There are two possible explanations. First, a crack in the oxide layer (as described above) [6] was observed in a specimen of polysilicon, and many trials on polysilicon have subsequently been carried out [7]. With many random grains overlapping each other, the identification of crystal defects generated by fatigue can be difficult in polysilicon. Additionally, defects can be essentially confined to quite small areas by grain boundaries. Second, even in the case of single-crystal silicon,

crystal defects have been investigated by transmission electron microscopy (TEM) in specimens that had been thinned for observation. However, thinning eventually shaves off part of the specimen, and that part may have been where the defects were generated. Evidence of defect accumulation has recently been captured by electron beam-induced current (EBIC) imaging [18, 19] without applying thinning. Even in the case of a sample that had been thinned for observation, dislocations that had possibly accumulated in advance were eventually observed with HVTEM in one of two specimens after fatigue fracture [20]. In that case, there must have been defects growing in the crystal, not just in the surface oxide, during fatigue.

In the present study, and in the context of the considerations described above, a new experiment was planned for the identification of crystal defects during fatigue. Our strategy was to investigate specimens of single-crystal silicon without applying any thinning, i.e., to examine entire specimens so that nothing would be missed. Therefore, 1 MeV HVTEM was used, which enables the investigation of silicon crystals that are up to $2\text{ }\mu\text{m}$ thick. This allowed the inspection of the entire thickness of the fatigue-loaded specimens. The details of the fatigue test and the subsequent investigations are described in order in the following sections.

Material and mechanical loading setup

A $2\text{-}\mu\text{m}$ -thick specimen was designed and fabricated into the configuration shown in Fig. 1a, as being integrated onto the loading structure. To confine the area of observation, the specimen was designed with notches for local stress concentration, as shown in Fig. 1b. It also had a small notch on one side with a radius of curvature of $5\text{ }\mu\text{m}$ for further stress concentration, as indicated in Fig. 1c. Actual fabrication was carried out using silicon on insulator (SOI) wafers manufactured by Semiconductor Wafer, Inc., Taiwan, which consisted of a $2\text{ }\mu\text{m} \pm 0.5\text{-}\mu\text{m}$ -thick device layer, a $0.8\text{ }\mu\text{m} \pm 0.5\%$ -thick buried oxide (BOX) layer, and a $200\text{ }\mu\text{m} \pm 10\text{-}\mu\text{m}$ -thick handle layer. The front and back surfaces comprised {100} oriented p-type single-crystal silicon and were mirror-polished. The electrical resistivity of the device layer and handle layer was $10\text{--}20\text{ }\Omega\text{cm}$. The specimen and the loading structure were made out of the

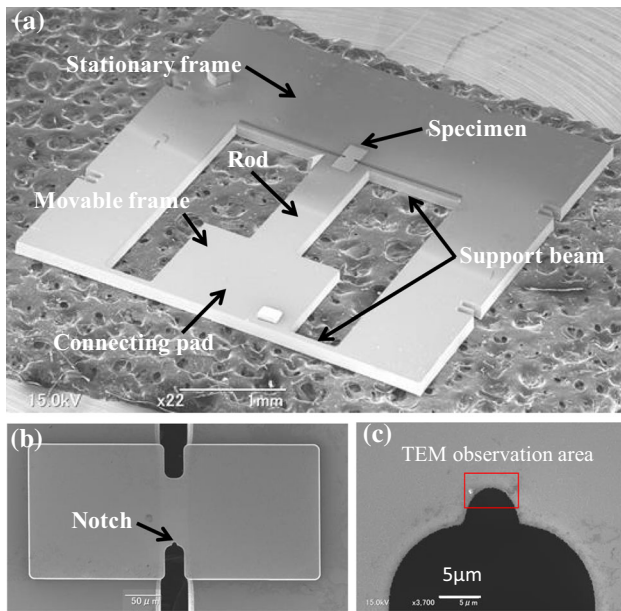


Figure 1 Scanning electron microscopy (SEM) images of micro-test structure and specimen fabricated by silicon on insulator (SOI) technology. **a**, The micro-test structure comprised a stationary frame and a movable frame. The thin film silicon specimen was integrally fabricated on the micro-test structure. **b**, Silicon thin film specimen (2 μm thick, 100 μm long, 26 μm wide). **c**, Oval notch on specimen for a stress concentration factor of 3.55; the area indicated by the red rectangle was investigated by high-voltage transmission electron microscopy (HVTEM).

device layer and handle layer, respectively, by applying both standard lithography and reactive ion etching (RIE).

The load was applied to the specimen through the loading structure while being installed on a holder for HVTEM observation. This was to facilitate the transfer between experiment and observation anticipating subsequent in situ experiments. The loading structure was 4.4 mm \times 4.4 mm square and consisted of a stationary outer frame and a movable inner frame, as shown in Fig. 1a. One end of the specimen was anchored with the remaining BOX layer to the stationary frame, and the other end was anchored to the movable frame, so that the load was transferred to the specimen when the movable frame was shifted by the external actuator. For the purpose of connecting the loading structure to an external actuator, the movable frame had a pad that was soldered to the silicon rod, which was then screwed onto the end of the loading train. The loading train, which coupled a piezoactuator (model P-841.20, travel 30 μm , resolution 0.6 nm, PI, Germany) and a

silicon rod with a load cell (model 9215, resolution 1 mN, stiffness 140 N/ μm , Kistler, Switzerland) in between, was assembled inside the HVTEM sample holder, as shown in Fig. 2a–c. Each experiment was carried out on the HVTEM sample holder, which was inserted in an environmental chamber (model TH441HA, accuracy ± 0.1 $^{\circ}\text{C}$ and $\pm 1\%$, ETAC, Japan) at 25 $^{\circ}\text{C}$ and 80% relative humidity (RH), as shown in Fig. 2d.

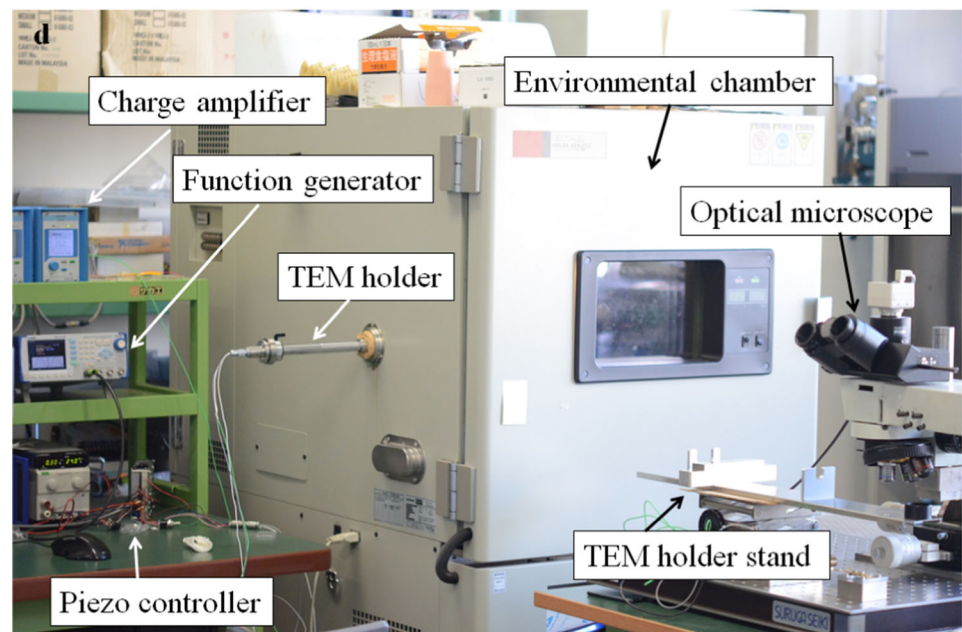
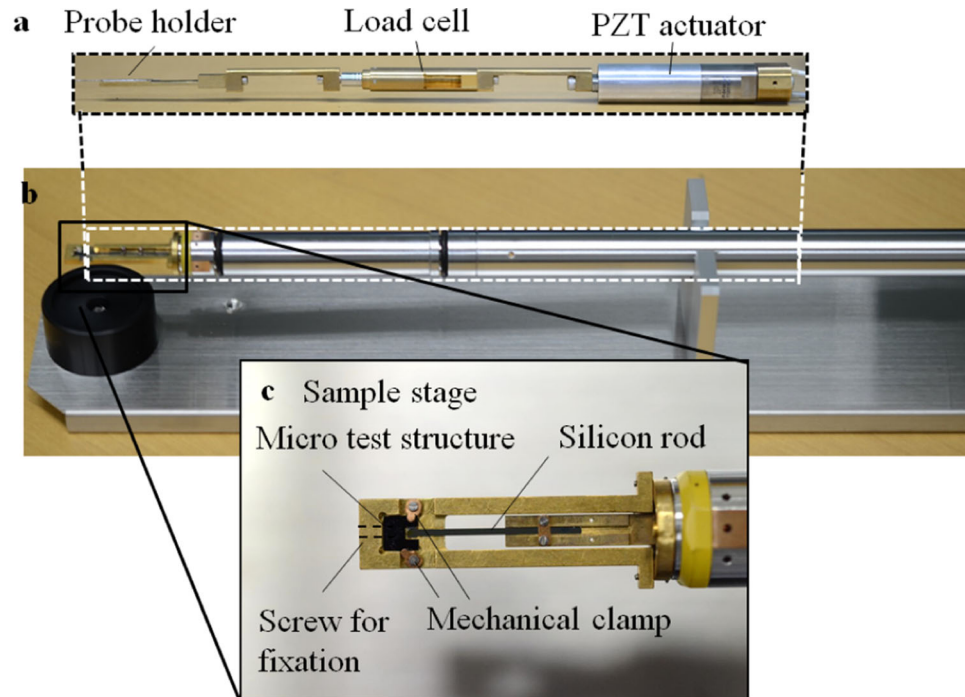
TEM observation

The specimen notch tips were subjected to investigation by HVTEM after fracture by a Reaction Science high-voltage scanning transmission electron microscope (model JEM-1000 K RS, maximum voltage acceleration 1000 kV, point resolution 0.15 nm, JEOL, Tokyo, Japan) at Nagoya University.

Results of fatigue test

As the first step, the stress amplitude level of the fatigue test was determined. This was accomplished by subjecting some of the specimens to static tensile tests to determine their strengths by applying a monotonically increasing load, and subjecting the remaining specimens to fatigue tests. Figure 3a shows an example of the load–displacement curve associated with the static tensile test. A sudden drop appears in the load, which corresponds to the load applied to the specimen immediately before fracture. The strength of each specimen, i.e., the stress applied at the notch tip when the specimen broke, was obtained using the commercial finite element analysis software ABAQUS on the basis of this drop in load [21], with the notch tip stress concentration and the thickness of the individual specimen taken into account. Figure 3b presents the distribution of strength, where the cumulative fracture probability was obtained by the mean rank method [22] and plotted along the ordinate with the applied stress along the abscissa. The average strength of the specimens was 2.53 GPa. The fitting curve represents the Weibull distribution [22], which is widely used to estimate the strength of brittle material and was optimized to the experimental data. The shape parameter m and the scale parameter σ_0 were

Figure 2 Experimental setup for loading specimen on the high-voltage transmission electron microscopy (HVTEM) sample holder. **a** Load cell and piezoelectric (PZT) actuator inside holder body for applying force to specimen. **b** Overview of transmission electron microscopy (TEM) holder body. **c** Close-up view of sample stage and mounted micro-test structure. **d** Environmental chamber assembled with the HVTEM holder for static and fatigue tests.



calculated as 6.65 and 2.65 GPa, respectively, which are within the ranges of other experimental data [23].

As the second step, a tension–compression fatigue test with a stress ratio $R = -1$ was carried out [24]. The stress amplitude level was set to within 80%–130% of the average strength. The frequency of the cyclic load in the fatigue test was set at 40 Hz. Figure 3c is a plot of the fatigue lifetime of the specimens, in which the stress amplitude normalized with

the average strength is plotted on the ordinate and the number of cycles to fracture is plotted on the abscissa. The fatigue lifetimes of the specimens were distributed within the range 10^5 – 10^7 cycles under a stress amplitude level of 80%–130% of the average strength, and once again they are in agreement with other common experimental data [25].

Unfortunately, many specimens shattered into pieces when they broke unstably. However, some

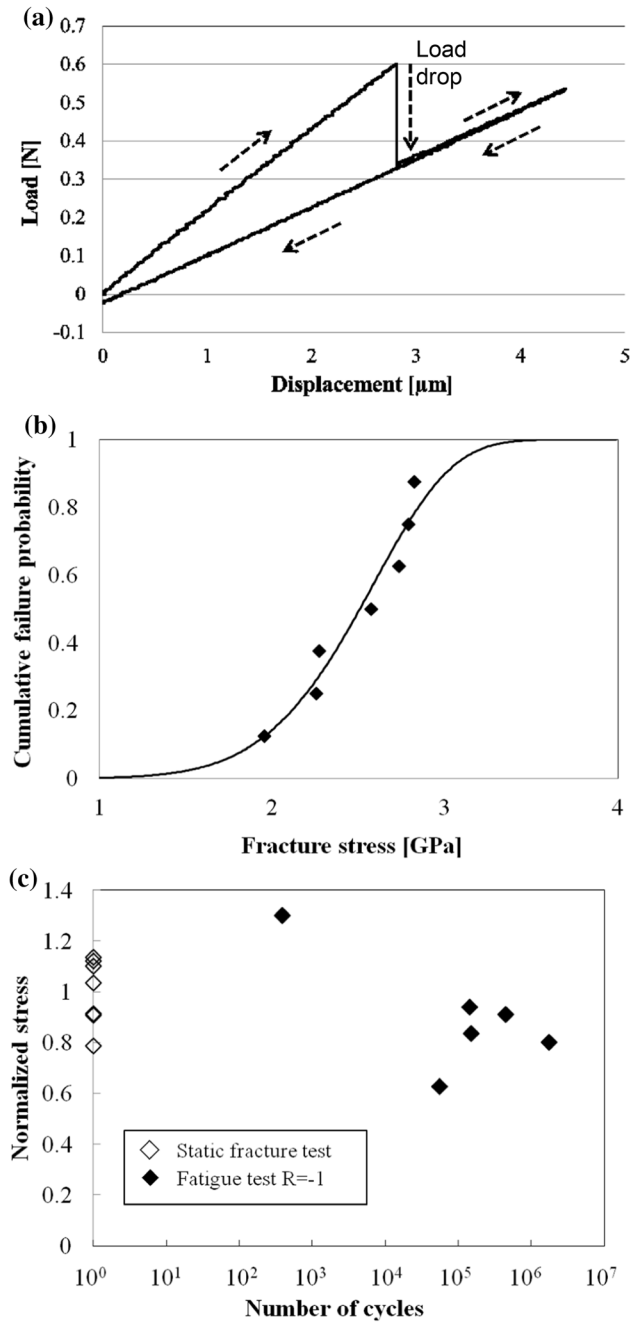


Figure 3 Results of static and fatigue tests at 25 °C and 80% relative humidity (RH). **a** Example of load (ordinate) versus displacement (abscissa) plot obtained from the static test. **b** Fracture stress plotted using the mean rank method; the fitting curve represents the Weibull distribution. **c** Fatigue lifetime data with the stress ratio $R = -1$.

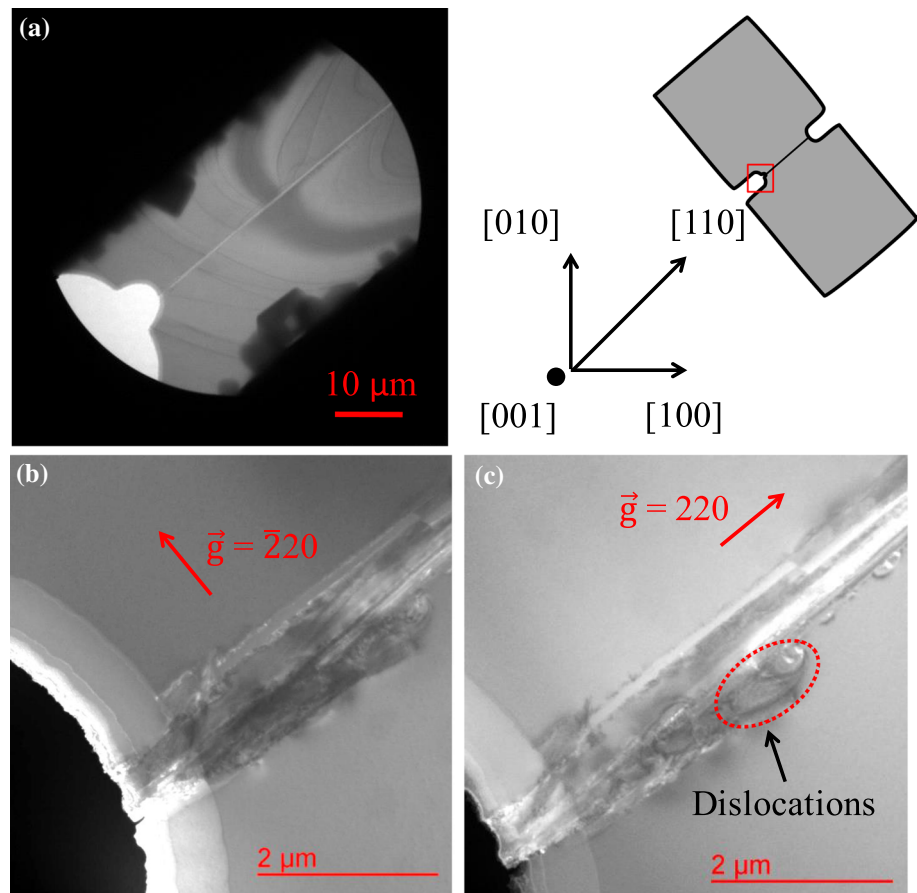
retained their original shape and were simply divided in two by a crack; these specimens were used for the HVTEM investigations.

Observation results

Figure 4 shows dark-field HVTEM images of the notch tip obtained from a specimen broken by a monotonically increased load. The images are intended for comparison with those of a fatigue fracture, which are shown later. Figure 4a shows a low-magnification HVTEM image of a broken specimen on the left side and an illustration of the entire specimen on the right side. The illustration shows the crystallographic orientations, and the red square indicates the region from which the magnified HVTEM images in Fig. 4b and c were obtained. They were obtained using weak-beam dark-field image contrast experiment [26] with diffraction vectors $\bar{2}20$ and 220 , as indicated over the images. The bright arc areas in the lower-left sides of the images are due to the partially thinned notch edge with scallops that formed during the etching process [27]. The bright, solid straight patterns running diagonally to the upper right corners of the figures, which did not alter with the diffraction vectors, probably correspond to a crack that emanated from a point along the notch tip and extended unstably to break the specimen in a brittle manner. Because the bright straight pattern has a certain width, and plural cracks hardly ever extend simultaneously from a mechanical perspective, it should be a single crack extending along $(1\bar{1}\bar{1})$ inclined to the specimen surface (001) . It is widely known that silicon has its slip planes along $\{111\}$ [28], and cleavage planes along $\{111\}$ and $\{110\}$, whose surface energies are close to each other (1.23 J m^{-2} and 1.51 J m^{-2} , respectively) [29]. In contrast, the ambiguous dark and hazy cloud-like patterns in Fig. 4b and c probably correspond to dislocations, judging from the fact that dislocations are invisible to TEM when the diffraction vector is perpendicular to the Burgers vector, and that parts of them appear and disappear depending on the diffraction vector. We speculate that dislocations were emitted from the crack as its extension was being accelerated unstably by the excess elastic energy.

Figure 5 shows bright-field HVTEM images of the notch tip obtained from a specimen broken by 4.49×10^5 cycles of fatigue loading at a stress level of 91.1% of the strength. As shown in Fig. 5a, an unstable crack appears to be extended in the same way as in Fig. 4, originating along the $(1\bar{1}\bar{1})$ plane and gradually shifting to extend along $(1\bar{1}0)$ in a long run,

Figure 4 Dark-field high-voltage transmission electron microscopy (HVTEM) images of the notch tip on the specimen after the static test. **a** Low magnification HVTEM image of the broken specimen (left), and illustration of specimen showing crystallographic orientations (right). **b** and **c** HVTEM images of notch tip under various diffraction conditions. Dislocation originating from an extending crack was observed around the fracture surface.



as schematically illustrated in Fig. 5b. As mentioned in the previous paragraph, in this case silicon slipped along $(1\bar{1}\bar{1})$ or $(1\bar{1}1)$ where the largest shear stress was applied, $(1\bar{1}0)$ was another potential cleavage plane. Therefore, in this situation the unstable crack extension may have started with slip deformation along $\{111\}$ and may subsequently have gradually shifted to the $\{110\}$ cleavage plane with just a little larger surface energy and a much larger tensile stress. A similar scenario may also hold for cases of fracture under monotonically increasing load, as shown in Fig. 4. In such cases, it is commonly recognized that initial defects induced by etching [30] determine the strength of the silicon structure, while possibly triggering unstable slip deformation to initiate crack extension along $\{111\}$. However, a number of shorter bright lines are also clearly visible in Fig. 5a that are not present in Fig. 4; they extended from different points along the notch edge, as illustrated in Fig. 5b. Furthermore, the lines are probably line defects emanating from points not on the extending crack but from directly along the notch edge apart from the

crack, because their appearance is significantly different from that of the vaguely cloud-like lines in Fig. 4. Therefore, the lines in Fig. 5a accumulated before the crack started its unstable extension.

Figure 6a and b shows dark-field images showing the weak-beam dark-field image contrast experiment, obtained from the same specimen shown in Fig. 5. Once again, because some corresponding parts of the line defects appear and disappear depending on the diffraction vectors, they must be edge dislocations. In comparison with the case of fracture under a monotonically increasing load shown in Fig. 4, these dislocations appear in more clearly defined triangular patterns, as indicated in Fig. 6b. The crystallographic orientations of the slip system and the expected direction of the dislocation line in silicon are illustrated in Fig. 7a. In comparison with the HVTEM image in Fig. 7b, which is a repeat of Fig. 5a, and the projection of the slip system illustrated in parallel in Fig. 7c, the triangles obviously spread along the $\{111\}$ slip plane confined within the two $\langle 110 \rangle$ slip directions. In particular, line defect C indicated in

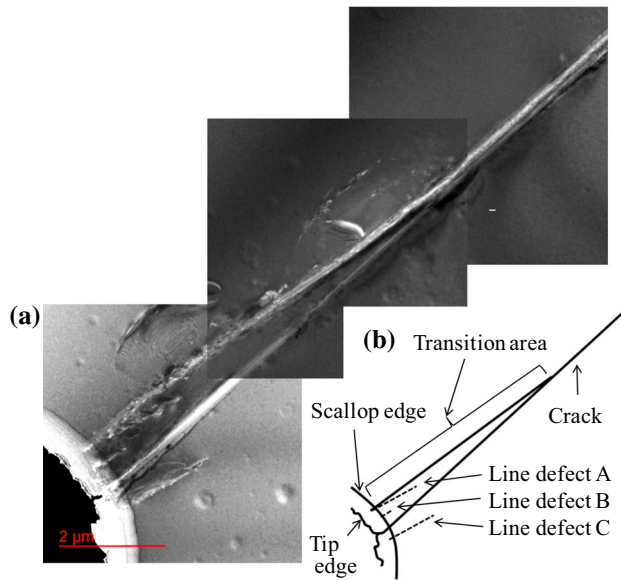


Figure 5 Bright-field high-voltage transmission electron microscopy (HVTEM) images of fractured specimen after fatigue test with $R = -1$. **a** Magnified view of the notch tip showing the crack extension and linear defects accumulated by mechanical loading. **b** Schematic representation of the notch tip on the fractured specimen.

Fig. 5b, which is also indicated in Fig. 6b by the white arrow, is located completely apart from the other defects in the image and does not intersect with the crack. Therefore, the lines appear to have been emitted and accumulated in a more stable manner, probably in advance of the activity of the unstable crack extension in the event of fatigue fracture to release the strain energy at a certain cycle of loading.

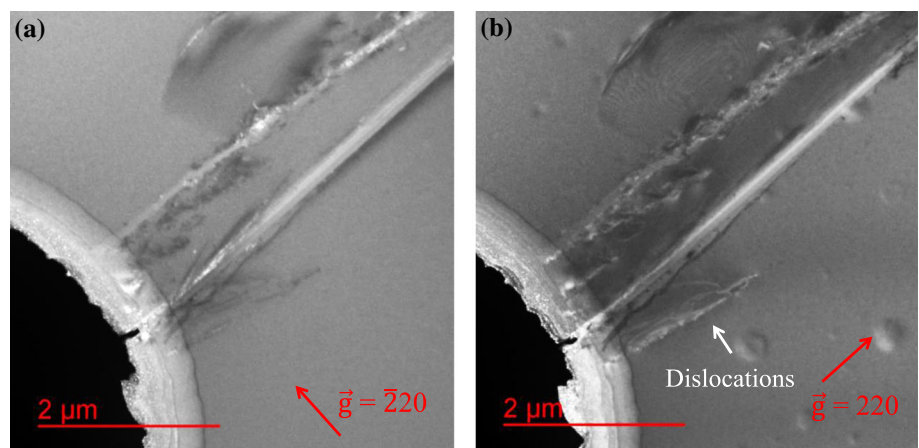
Another case of such a situation is shown in Fig. 8a and b, which are similar dark-field images obtained from a different specimen fatigue-fractured at a stress

amplitude level of 62.9% after 5.47×10^5 cycles. Again, a trace of subcritical dislocation accumulation is clearly visible in the triangles apart from the crack that broke the specimen. These multiple observations indicate an essential scenario for fatigue fracture in silicon, as follows. Dislocations such as those shown in Figs. 5, 6, and 8 accumulate along the {111} slip planes, starting from the initial defects induced by etching [30], and progress in a number of small local areas along the region of stress concentration under cyclic fatigue loading. Such defect accumulation induces further local stress concentration, thereby reducing the remaining strength of the material. After a certain number of fatigue cycles, an unstable crack extension starts from the most severely stressed and weakened area along the same {111} plane. The evidence for this scenario is discussed in the next section.

Discussion of the fatigue process

In crystalline silicon structures, the fatigue process starts with the initial defects induced by machining, i.e., mostly etching [30], which commonly occur during the fabrication of MEMS structures. After a certain number of fatigue loading cycles, such crystal defects are restructured into dislocations. This is assisted by concentrated local stress, for example, at the notch tip. The dislocations then induce further stress concentration, which causes further dislocations. This positive feedback accelerates concentrated defect accumulation, resulting in highly organized defect structures with dislocations that are densely distributed along a slip plane, as illustrated in Figs. 6

Figure 6 Dark-field high-voltage transmission electron microscopy (HVTEM) images showing edge dislocation near fatigue crack origins in specimens. Figures **a** and **b** show the same specimen shown in Fig. 4.



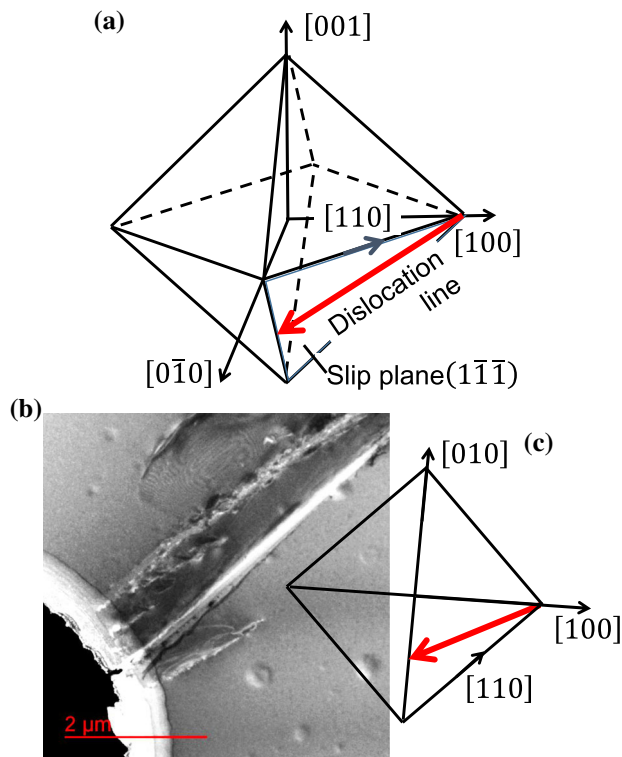


Figure 7 Crystallographic orientation and slip system of each specimen. **a** One of the slip planes with the largest resolved shear stress and the expected direction of the dislocation line. Part of Fig. 5 is presented here as **b** next to the slip system **c** projected onto the specimen surface [001].

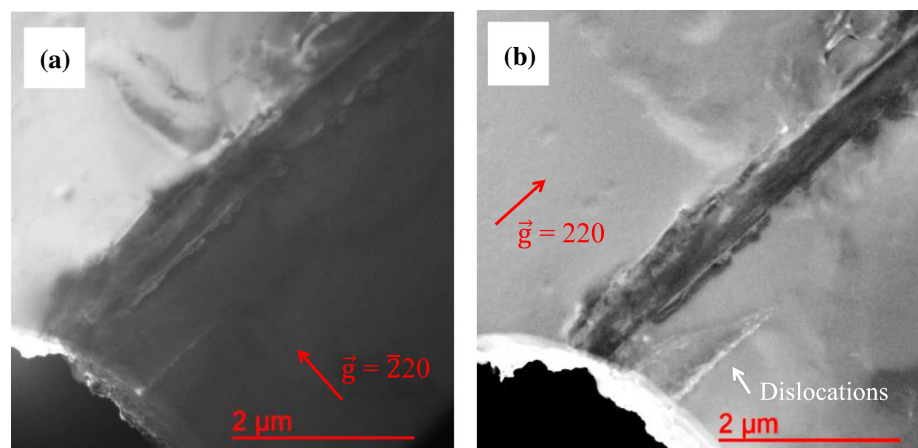
and 8. These accumulated defects appear completely different from those in Fig. 4, which were induced by sudden unstable crack extension with excess strain energy in a static fracture test.

After accumulation on a slip plane, a number of dislocations may move out onto the notch surface. This stage probably corresponds to the slip band and

extrusion/intrusion commonly observed in the fatigue of metallic materials. The incubation of fatigue-crack embryos begins then and may lead to a certain degree of stable crack extension. Traces of such stable fatigue crack extensions have been observed on the fracture surfaces of large-scale specimens [20], with striation-like patterns that commonly appear in metallic materials. However, because the number of line markings was so small (less than ten) [20], such a crack would have stably extended for just several cycles before unstable fracture. Therefore, it may have proceeded almost immediately to the catastrophic unstable extension of a macroscopic crack. Once a macroscopic crack extends, its original crystal slip plane with accumulated dislocations is assimilated into the large crack surface and is hardly discernible by post-mortem TEM, no matter how high the magnification.

In contrast, the first part of the fatigue process mentioned above, i.e., from etching damage to the accumulation of dislocations on a slip plane, takes much longer, which is probably analogous to the situation in metallic materials. As commonly seen in metallic materials, many slip bands and extrusions/intrusions originate at the beginning of the fatigue process. This is because their growth is so slow that the time windows of the individual growth processes overlap with each other. In contrast, usually only one fatigue crack extends from one of those intrusions. This is because the cracks extend relatively quickly toward the final fracture, so the possibility of more than one process overlapping is practically zero. Particularly in brittle materials such as silicon, it is easy to imagine the latter half of the fatigue process, i.e., from crack nucleation to unstable fracture, to

Figure 8 Another case of similar defect accumulation observed in a different specimen from that in Fig. 6.



proceed much more quickly than in less brittle materials. Therefore, even stable fatigue crack extension processes are practically unidentifiable, whereas plural defect accumulation sites remain after unstable fractures. Therefore, the observed results, in which plural slip sites were found but only one unstable crack was identified without any trace of stable crack extension (Figs. 5, 6, and 8), strongly support the scenario proposed above. Accordingly, although further detailed analysis is necessary to determine the structure and behavior of accumulated dislocations, we strongly suspect that the essential origin of fatigue fracture in silicon is somewhat more metallic in nature than previously supposed.

Conclusions

In the present study, we developed and assembled a microscale test structure comprising a 2- μm -thick single-crystal silicon specimen and a HVTEM sample holder with a mechanical loading apparatus to determine the fatigue mechanism of silicon. HVTEM was used to investigate the entire thickness of the specimen after fatigue fracture, i.e., without any post-fracture thinning. A number of linear defect contrasts, which were confirmed as edge dislocations by weak-beam dark-field image contrast experiment, emanated from the edge of the stress concentration notch apart from the unstably extended crack that broke the specimen. The results revealed that edge dislocations were generated, accumulated, and extended along the {111} crystal slip plane during fatigue loading before unstable brittle fracture. This strongly implies that the mechanical fatigue fracture of silicon is due to crystal slips. Therefore, silicon may behave more like a metal in fatigue than previously suspected.

Acknowledgements

This work was partly supported by the Nanotechnology Platform Program from the Ministry of Education, Culture, Sports, Science, and Technology, Japan, and by a Grand-in-Aid for Scientific Research from the Japan Society for the Promotion of Science. The HVTEM investigations were carried out at the High-Voltage Electron Microscope Laboratory, Eco-Topia Science Institute, Nagoya University, Japan.

This work was partly funded by a Grant-in-Aid for Scientific Research from the Japan Society for the Promotion of Science (grant number 19K4091).

Declarations

Conflict of interest The authors declare that they have no conflicts of interest.

References

- [1] Connally JA, Brown SB (1992) Slow crack growth in single-crystal silicon. *Science* 256:1537–1539
- [2] Kahn H, Ballarini R, Bellante JJ, Heuer AH (2002) Fatigue failure in polysilicon not due to simple stress corrosion cracking. *Science* 298:1215–1218
- [3] Bagdahn J, Sharpe WN (2003) Fatigue of polycrystalline silicon under long-term cyclic loading. *Sens Actuators A* 103:9–15
- [4] Ikehara T, Tsuchiya T (2008) High-cycle fatigue of micro-machined single-crystal silicon measured using high-resolution patterned specimens. *J Micromech Microeng* 18:075004
- [5] Brede M (1993) The brittle-to-ductile transition in silicon. *Acta Metall Mater* 41:211–228
- [6] Muhlstein CL, Stach EA, Ritchie RO (2002) A reaction-layer mechanism for the delayed failure of micron-scale polycrystalline silicon structural films subjected to high-cycle fatigue loading. *Acta Mater* 50:3579–3595
- [7] Alsem DH, Timmerman R, Boyce BL, Stach EA, Hosson JTM, Ritchie RO (2007) Very high-cycle fatigue failure in micron-scale polycrystalline silicon films: Effects of environment and surface oxide thickness. *J Appl Phys* 101:013515
- [8] Asaoka K, Umeda T, Arai S, Saka H (2005) Direct evidence for shuffle dislocations in Si activated by indentation at 77 K. *Mater Sci Eng A* 400–401:93–96
- [9] Okuno T, Saka H (2013) Electron microscope study of dislocations introduced by deformation in a Si between 77 and 873 K. *J Mater Sci* 48:115–124
- [10] Nakao S, Ando T, Shikida M, Sato K (2008) Effect of temperature on fracture toughness in a single-crystal-silicon film and transition in its fracture mode. *J Micromech Microeng* 18:015026
- [11] Namazu T, Isono Y, Tanaka T (2002) Plastic deformation of nanometric single crystal silicon wire in AFM bending test at intermediate temperatures. *J Microelectromech Syst* 11:125–135
- [12] Yamaguchi H, Tatami J, Yahagi T, Nakano H, Iijima M, Takahashi T, Kondo T (2020) Dislocation-controlled

- microscopic mechanical phenomena in single crystal silicon under bending stress at room temperature. *J Mater Sci* 55:7359–7372
- [13] Oestlund F, Rzepiejewska-Malyska K, Leifer K, Hale LM, Tang Y, Ballarini R, Gerberich WW, Michler J (2009) Brittle-to-ductile transition in uniaxial compression of silicon pillars at room temperature. *Adv Funct Mater* 19:2439–2444
- [14] Dehm G, Jaya BN, Raghavan R, Kirchlechner C (2018) Overview on micro- and nanomechanical testing: new insights in interface plasticity and fracture at small length scales. *Acta Mater* 142:248–282
- [15] Marabet A, Texier M, Tromas C, Brochard S, Pizzagalli L, Thilly L, Rabier J, Talneau A, Vaillant YM, Thomas O, Godert J (2018) Low-temperature intrinsic plasticity in silicon at small scales. *Acta Mater* 161:54–60
- [16] Chen M, Pethoe L, Sologubenko AS, Ma H, Michler J, Spolenak R, Wheeler JM (2020) Achieving micron-scale plasticity and theoretical strength in silicon. *Nat Commun* 11:2681
- [17] Kato NI, Nishikawa A, Saka H (2001) Dislocations in Si generated by fatigue at room temperature. *Mater Sci Semicond Proc* 6:113–115
- [18] Kamiya S, Kita T, Izumi H (2014) Defect accumulation and strength reduction in single crystalline silicon induced by cyclic compressive stress. *Sens Actuators A* 208:30–36
- [19] Kamiya S, Kongo A, Sugiyama H, Izumi H (2018) Electronic imaging of subcritical defect accumulation in single crystal silicon under fatigue loading. *Sens Actuators A* 279:705–711
- [20] Kamiya S, Udhayakumar A, Izumi H, Koiwa K (2016) Shear stress enhanced fatigue damage accumulation in single crystalline silicon under cyclic mechanical loading. *Sens Actuators A* 244:314–323
- [21] Kamiya S, Ikeda Y, Gaspar J, Paul O (2011) Effect of humidity and temperature on the fatigue behavior of polysilicon thin film. *Sens Actuators A* 170:187–195
- [22] Weibull W (1951) A statistical distribution function of wide applicability. *J Appl Mech* 18:293–297
- [23] Tsuchiya T (2005) Reliability Characterization of MEMS Materials. *IEEE Transactions on Sensors and Micromachines* 125:289–293
- [24] Suresh S (1998) *Fatigue of materials*. Cambridge University Press, Cambridge, pp 224–227
- [25] Kamiya S, Tsuchiya T, Ikehara T, Sato K, Ando T, Namazu T, Takashima K (2011) In: 24th IEEE international conference on micro electro mechanical systems (MEMS 2011). pp 404–407
- [26] Hirsch PB, Howie A, Nicholson RB, Pashley DW, Whelan MJ (1965) *Electron microscopy of thin crystals*. Butterworth & Co Publishers Ltd., pp 162–193
- [27] Chang C, Wang YF, Kanamori Y, Shih J, Kawai Y, Lee C, Wu K, Esashi M (2005) Etching submicrometer trenches by using the Bosch process and its application to the fabrication of antireflection structures. *J Micromech Microeng* 15:580–585
- [28] Robert H (1999) *Properties of crystalline silicon*. The Institution of Engineering and Technology, London, pp 144–148
- [29] Jaccodine RJ (1963) Surface Energy of Germanium and Silicon. *J Electrochem Soc* 110:524–527
- [30] Schaefer S, Ludemann R (1999) Low damage reactive ion etching for photovoltaic applications. *J Vac Sci Tech A* 17:749–754

Publisher's Note Springer Nature remains neutral with regard to jurisdictional claims in published maps and institutional affiliations.